Fluid Phase Equilibria 581 (2024) 114077

Contents lists available at ScienceDirect

Fluid Phase Equilibria

journal homepage: www.journals.elsevier.com/fluid-phase-equilibria

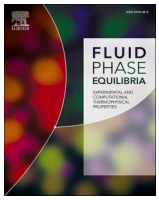

Thermodynamic Analysis of the Absorption of Common Refrigerants in Fluorinated Deep Eutectic Solvents

Merve Gözdenur Demirbek [a], Sabrina Belén Rodriguez Reartes [a,b,c], Fèlix Llovell [a,*]

[a] Department of Chemical Engineering. Universitat Rovira i Virgili, Avinguda dels Països Catalans, 26 – Campus Sescelades, Tarragona, 43007, Spain
[b] Departamento de Ingeniería Química, Universidad Nacional del Sur (UNS), Avda. Alem 1253, Bahía Blanca, 8000, Argentina
[c] Planta Piloto de Ingeniería Química – PLAPIQUI (UNS-CONICET), Camino "La Carrindanga" Km 7, Bahía Blanca, 8000, Argentina

ARTICLE INFO

KEYWORDS:
Fluorinated Deep Eutectic Solvents
Hydrofluorocarbons
soft-SAFT
solubility
selectivity

ABSTRACT

The potential to decrease the negative environmental impact of greenhouse gases in terms of global warming potential (GWP) is a current challenge. Apart from CO_2, fluorinated greenhouse gases (F-gases), which are human-made chemicals used in refrigeration and other industrial applications, have a huge environmental impact due to their high GWPs. In this regard, the design of units to capture and recover these gases would contribute to their reuse, avoiding the negative impact of their final emission or incineration. Fluorinated Deep Eutectic Solvents (FDESs) have been considered as promising solvents for the absorption and the selective separation of F-gases. However, the complex and expensive experimental labour to fully characterize FDESs delays its study and development. In this work, a computational approach is applied to develop accurate thermodynamic models of the gas solubility of several F-refrigerants in DESs. The molecular-based equation of state (EoS) soft-SAFT is used to assess the absorption of three F-gases (1,1,1,2-tetrafluoroethane (R-134a), difluoromethane (R-32), and pentafluoroethane (R-125)) at different temperatures in five DESs derived from fluorinated salts and perfluorinated acids. New molecular models are developed through the soft-SAFT approach for FDESs in good agreement with experimental data, and the solubility of F-gases is also calculated at varying temperatures with high accuracy. Then, an in-depth analysis of the characteristics of the refrigerants, and of the FDESs affecting the F-gases absorption is performed, and the enthalpy and entropy of absorption and the selectivity are calculated. It has been encountered that the best FDESs for each particular F-gas separation can be obtained by modifying the composition of DES and the operating temperature. Finally, an assessment based on the selectivity obtained from the soft-SAFT model is carried out to choose the most adequate solvent to separate the studied F-gases.

1. Introduction

Global warming and shifts in weather patterns are driving climate change on Earth, marked by an increase in the average global temperature [1] and the occurrence of extreme weather events, such as wildfires, droughts, and other natural disasters. Increased levels of greenhouse gases (GHGs) in the atmosphere are considered the main cause for global warming, and these gases are primarily originated by human activities, such as the burning of fossil fuels, intensive refrigeration, or agriculture. Although GHGs are typically identified with carbon dioxide (CO_2), there are other relevant substances with significant impact that also deserve attention.

GHG emissions in 2021 in the European Union were 79.1% carbon dioxide, 12.8 % methane, 5.7% nitrogen oxide, and 2.4 % fluorinated gases (F-gases) [2]. While the emissions of these F-gases make up a relatively small percentage of total emissions, their impact on global warming potential (GWP) can be up to four orders of magnitude times greater than that of CO_2. It is anticipated that their effect could lead to a 0.5°C increase in the Earth's global temperature by 2050 if no actions are taken [3]. In this regard, it is worth to mention the efforts of the European Union which, since 2017, is reducing F-gases interannual emissions, with a remarkable 5% reduction in comparison to 2020 [2].

F-gases are synthetic GHGs, including hydrofluorocarbons (HFCs), perfluorocarbons (PFCs) and sulfur hexafluoride (SF_6), mostly used in air conditioning, refrigeration, insulation, and energy sector applications [4]. While the Montreal Protocol [5] encouraged the phase-out of

* Corresponding author:
E-mail address: felix.llovell@urv.cat (F. Llovell).

https://doi.org/10.1016/j.fluid.2024.114077
Received 7 December 2023; Received in revised form 9 February 2024; Accepted 7 March 2024
Available online 8 March 2024

earlier ozone-depleting (ODP) substances in refrigeration devices, such as chlorofluorocarbons (CFCs) and hydrochlorofluorocarbons (HCFCs), this action consequently led to the exponential increase in the use of HFCs for this purpose. The HFCs substitutes, even without damaging the ozone layer, have elevated GWPs that contribute to climate change, posing a new challenge for the planet's sustainability [6]. Indeed, as cooling services needs are estimated to continue increasing, the HFC emissions will consequently augment if mitigation actions are not taken, particularly in emerging countries [7].

In order to regulate HFC consumption, the Kigali Amendment to the Montreal Protocol was signed in 2016 and came into effect in 2019, establishing an international framework for that end [6]. The European Union (EU) regulation (EU No. 517/2014) is also in force, aiming for a 60% reduction of F-gases emissions by 2030 [3], based on the baseline year 2005. In this regard, two different paths are currently being explored. From one side, several studies are focused on the replacement of current refrigerant mixtures by new systems with similar technical properties but lower environmental impact. From the other side, a mid-term solution is to increase the recyclability of these compounds, avoiding the current linear economy model, where F-gases are not reused, being sent to incineration after the end-of-life of the equipment. To accomplish this goal, adequate separation technologies need to be designed, as most gases are found in blends, where only one of the compounds can be recycled. Separation technologies have been studied in the literature, either using adsorption with activated carbons [8–11], membrane separation processes [12] or proposing absorption through Ionic Liquids (ILs) [13–22].

Within the context of absorption techniques, Deep Eutectic Solvents (DESs) have recently emerged as potential solvents for sharing many common properties with the ILs. DESs are mixtures of two or more substances, typically a salt and a neutral complexing agent, whose solid-liquid transition temperature decreases considerably compared to that of the corresponding ideal mixture. This feature arises from the strong hydrogen bond network formed between the components: a hydrogen bond donor (HBD) and a hydrogen bond acceptor (HBA). DESs are non-volatile and very tuneable, offering a wide range of options for multiple applications, including separation processes for gas capture [23,24], among others. However, while most studies are related to CO_2, their application to F-gases absorption remains limited [25,26].

Codera et al. [25] have studied the solubility of refrigerants R-32, R-125, R-134a, and R-143a in several Choline Chloride-based DESs, including ethylene glycol and glycerol as HBDs. The results showed low solubility in these DESs, even though there were remarkable differences between the HFCs, providing a promising selectivity for separation. One possible way to improve the solubility of DESs consists on adding fluorine atoms, either to the HBA or the HBD. This assumption is based on previous contributions on the use of fluorinated ionic liquids (FILs), which have been shown to present three nano-segregated domains (fluorinated, nonpolar, and polar), providing these fluids with unique properties and increasing their solubility power [27]. In particular, FILs have demonstrated promising results in terms of F-gas solubility [13,28,29].

Based on these results, it is interesting to explore the potential of using DESs derived from FILs and combined with perfluorinated acids. In a preliminary study performed by Castro et al. [26], some new DESs were formed using salts composed of cations with various structures (imidazolium, cholinium, tetrabutylammonium) combined with different perfluorinated anions of varying chain lengths (4-carbon or 8-carbon chains), and molecular structures (including sulfonate or carboxylate functional groups), mixed with fluorinated carboxylic acids. A thermophysical characterization was carried out in terms of density of tetrabutylammonium perfluorobutanesulfonate $[N_{4444}][C_4F_9SO_3]$, 1-Ethyl-3-methylimidazolium perfluorooctanesulfonate $[C_2C_1Im][C_8F_{17}SO_3]$ (2-Hydroxyethyl)trimethylammonium perfluorobutanesulfonate $[N_{1112(OH)}][C_4F_9SO_3]$, (2-Hydroxyethyl)trimethylammonium perfluoro pentanoate $[N_{1112(OH)}][C_4F_9CO_2]$, and (2-Hydroxyethyl) trimethylammonium perfluorooctanesulfonate $[N_{1112(OH)}][C_8F_{17}SO_3]$ salts combined with n-perfluoropentanoic acid ($C_4F_9CO_2H$) and n-perfluorobutanesulfonate acid ($C_4F_9SO_3H$). Then, the absorption of three common F-gases used in refrigeration, 1,1,1,2-tetrafluoroethane (R-134a), difluoromethane (R-32), and pentafluoroethane (R-125), was experimentally studied in a range of temperatures between 303.15 and 323.15 K. The results showed that it was possible to achieve elevated solubility at low-pressure conditions. However, the dependence on the appropriate cation-anion choice in the salt and the fluorinated acid, including the proportion between both compounds, have a strong impact on the final capacity of each solvent, affecting the selection of the most proper DESs for a particular separation. Hence, computational tools are of great help to screen and select new FDESs, reducing the experimental effort required in the characterisation of these compounds. In this work, new accurate thermodynamic models are developed to characterise the absorption of F-refrigerants in these FDESs through the molecular-based soft-SAFT equation of state (EoS), a mature version of the original SAFT [30,31]. The successful soft-SAFT variant [32] has been used in this study, based on the excellent results obtained for systems with ILs [20,33–40] and DESs [41–45]. As far as hydrogen bonding and association interactions are specifically treated in one term of the equation, a more realistic description of DESs, compared to classical cubic EoSs, is obtained.

After proposing a suitable molecular model for different FDESs using the soft-SAFT approach, a complete thermodynamic characterisation is performed using an individual-component approach, where each compound in the DESs has its own molecular parameters. Then, the solubility of R-134a, R-32, and R-125 refrigerants is assessed for two selected DESs at 303.15, 313.15, and 323.15 K, and pressures up to 1 MPa. A discussion on the effect of HBA:HBD ratio, the temperature, type of F-gas, and type of salt is carried out. Finally, the soft-SAFT is used to predict the enthalpy and entropy of absorption and to evaluate the selectivity, allowing to identify the best DESs for each particular F-gas separation.

2. Theory

The Statistical Associating Fluid Theory (SAFT) [30,31], and its different incarnations, are a group of EoSs based on Wertheim's first-order thermodynamic perturbation theory (TPT1) [46–48], that explicitly account for the effect of hydrogen bonding. Their mathematical expression is set in terms of the residual Helmholtz energy, A^{res}, of the system, calculated as a sum of contributions [Eq. (1)]:

$$A^{res} = A - A^{id} = A^{ref} + A^{chain} + A^{assoc} \quad (1)$$

where A^{id} is the ideal gas term, and A^{ref} is the reference contribution to the Helmholtz energy, which describes the monomer-monomer interactions according to an intermolecular potential. In this work, the soft-SAFT variant developed by Blas and Vega [32], and Pàmies and Vega [49] is used, hence a Lennard-Jones (LJ) fluid is taken for the reference term of the equation. The LJ potential is defined by a characteristic segment diameter, σ, and dispersive energy, ε. A^{ref} term is calculated through the correlation of Johnson [50] fitted to LJ simulation data. As far as there is not an equivalent expression for mixtures, the van der Waals one-fluid theory is used [51]. For this purpose, it is necessary to extend the molecular parameters using the so-called modified Lorentz-Berthelot (LB) combining rules:

$$\sigma_{ij} = \eta_{ij}\left(\frac{\sigma_{ii} + \sigma_{jj}}{2}\right) \quad (2)$$

$$\varepsilon_{ij} = \xi_{ij}\left(\varepsilon_{ii}\varepsilon_{ij}\right)^{1/2} \quad (3)$$

where η_{ij} and ξ_{ij} are size and energy binary parameters, typically fitted to mixture data. When no mixture data is used, these values are set to one

(or transferred from a similar molecule). Note that $\xi_{ij} = (1- \underline{k_{ij}})$ in classical cubic EoSs.

In addition, Wertheim's TPT1 theory comprises A^{chain} and A^{assoc} terms, which account for chain connectivity and association interactions (hydrogen bonding), respectively. The A^{chain} and A^{assoc} terms are formally identical in all SAFT equations, as shown in Eqs (4) and (5):

$$A^{chain} = RT \sum_i x_i(1 - m_i) \ln g_{ij}^{LJ} \quad (4)$$

$$A^{assoc} = RT \sum_i x_i \sum_\alpha \left(\ln X_{\alpha,i} - \frac{X_{\alpha,i}}{2} \right) + \frac{M_i}{2} \quad (5)$$

It is important to note that g^{LJ} refers to the radial distribution function of the monomer-monomer interactions, while X_α refers to the fraction of molecules not bonded at a site. A detailed description of the equation can be found in [32]. In summary, a total of five molecular parameters characterize an associating molecule: m, the chain length; σ, the segment diameter; ε/k_B, the dispersive energy between segments defined following the LJ potential; and the site–site association energy, ε^{HB}/k_B, and bonding volume, K_{HB}, used to mimic hydrogen bonding and other directional short-range forces by including square-well spheres embedded into the core of the LJ segment.

3. Molecular Models

A proper description of the thermodynamic properties of a system requires the selection of a representative model for each molecule. In this work, hydrofluorocarbons (HFCs) are defined as homonuclear chainlike molecules with two association sites representing the polar interactions caused by the fluorine electronegativity. This model has been successfully used for determining the refrigerants' thermodynamic properties [52], as well as its behaviour with ILs and DESs [20,33,40,53], by means of the soft-SAFT approach, and has been adopted in this work for consistency with previous ones. Thus, the molecular parameters for R-32, R-134a and R-125 were directly transferred from Asensio-Delgado et al. [33] and Albà et al. [54] without any refinement.

Concerning the DESs studied in this work, both compounds forming the eutectic mixture are treated as independent entities. Consequently, the salt and the acid-forming DES have an individual model for each one. The "individual-component approach" has proven to be a robust and transferable framework for modelling DESs, being applied to different versions of SAFT, such as PC-SAFT [55] or soft-SAFT [42]. It provides a realistic and physically consistent method for keeping the molecular nature of each constituent of the DES. As a consequence, an independent set of molecular parameters for each component is fitted to experimental data, with the possibility of adding binary interaction parameters to account for any deviations in size or energy between both molecules. Additionally, when modelling gas solubility in DES, binary interaction parameters between each component and the gas may be required to accurately represent this solubility.

Then, an additional computational tool, Avogadro software [56], is used in this work to analyse the charge distribution and set the proper association sites of the molecules, as shown in **Figure S1** in the Supplementary Information.The modelling of the fluorinated salts is done based on the assumption that the cation and the anion are considered as an associating single-chain molecule, using the so-called ion pair assumption, based on previously successful results obtained for ILs with this approximation within the soft-SAFT framework [20,33,40,53]. However, it is important to account for the electric charge delocalisation in the anion due to the presence of fluorine atoms. In order to represent this delocalisation, $[N_{4444}][C_4F_9SO_3]$, $[C_2C_1Im][C_8F_{17}SO_3]$ $[N_{1112(OH)}][C_4F_9SO_3]$, $[N_{1112(OH)}][C_4F_9CO_2]$ and $[N_{1112(OH)}][C_8F_{17}SO_3]$ are modelled with a three-site association scheme: one main site called *A* to describe the main atom interaction of the cation with the anion, and two sites *B* to represent the delocalised charge because of the enclosing fluorine and oxygen atoms of the anion. Following the same strategy as done for previous contributions [38,53], only *AB* interactions are allowed in these models, i.e., when considering the interaction between two salt molecules. The structural differences between the salts will be effectively taken into account in the parametrisation of soft-SAFT molecular parameters. The sketch of interaction used to model the salts within the soft-SAFT is shown in **Figure S2** in the Supplementary Information.

Concerning $[HC_4F_9SO_3]$ and $[HC_4F_9CO_2]$, their carboxylic acid nature suggests the possibility of modelling them with only one associating site to mimic the formation of dimers, which is typical of these fluids. However, other authors [57] have noticed that, in aqueous solutions of carboxylic acids, a large number of water molecules are expected to bond to (solvate) the carboxylic acid group (COOH). Consequently, a higher number of sites were incorporated to reflect the formation of these clusters, using a three-sites approach (one *A* site for the doubly bonded oxygen and two sites *A* and *B* for the hydroxyl group). Thus, the soft-SAFT coarse-grain models of the carboxylic acids that were already available from the previous contribution of Jovell et al. [53] are used here in a transferable manner.

The parametrisation strategy of the proposed DESs is based on fitting the molecular parameters to DESs density experimental data at different temperatures at atmospheric pressure [26], using all HBA:HBD ratios simultaneously to obtain a composition-independent set of parameters. Given the fact that the parameters of the HBDs are known, only the parameters of the HBAs are obtained. This is done here for the first time for the fluorinated salts $[N_{4444}][C_4F_9SO_3]$, $[C_2C_1Im][C_8F_{17}SO_3]$, $[N_{1112(OH)}][C_4F_9SO_3]$, $[N_{1112(OH)}][C_4F_9CO_2]$, and $[N_{1112(OH)}][C_8F_{17}SO_3]$. A summary of the fitting procedure carried out is shown in Fig. 1.

The final list of soft-SAFT molecular parameters for all compounds involved in this work can be found in Table 1.

4. Results and Discussion

4.1. Density

The temperature-density description for $[N_{4444}][C_4F_9SO_3]$:$[HC_4F_9CO_2]$ (named DES A) and $[C_2C_1Im][C_8F_{17}SO_3]$:$[HC_4F_9CO_2]$ (named DES B) at different compositions are plotted in Fig. 2a and 2b, respectively. As it can be seen, no parameter degeneracy is observed when changing the proportion in the eutectic mixture, allowing a description of a different ratio using a single set of parameters without binary adjustments. Results of similar accuracy are displayed in Fig. 2c for a single (1:1) proportion for $[N_{1112(OH)}][C_4F_9SO_3]$:$[HC_4F_9CO_2]$ = DES C, $[N_{1112(OH)}][C_4F_9CO_2]$:$[HC_4F_9SO_3]$ = DES D, and $[N_{1112(OH)}][C_8F_{17}SO_3]$:$[HC_4F_9CO_2]$ = DES E.

4.2. Solubility of F-Gases in DESs

After validating appropriate molecular models for the new DESs, we proceed to describe the solubility of R-134a, R-32, and R-125 refrigerants in them. It is noteworthy that, among the five considered FDESs, $[N_{4444}][C_4F_9SO_3]$:$[HC_4F_9CO_2]$ and $[C_2C_1Im][C_8F_{17}SO_3]$:$[HC_4F_9CO_2]$ are the only ones with available experimental solubilities at different HBA:HBD ratios. For DES C, D, and E, solubility data are exclusively available at a 1:1 ratio. It is crucial to emphasize that, given the individual-component approach adopted for modelling FDESs, the refrigerant's solubility is treated within the context of a ternary mixture. This approach necessitates knowledge of all possible binary interactions occurring in the system. Although soft-SAFT can qualitatively explain the behaviour of these mixtures, quantitative agreement with the binary systems' accessible data is required to fully assess the validity of these DESs for separation purposes. As a result, two binary temperature-independent parameters, ξ and η (see Eqs. 2 and 3) are utilised to characterize the interaction between the HBA (salt) part of the DES and the refrigerant (R-32, R-125, and R-134a). This approach aims to

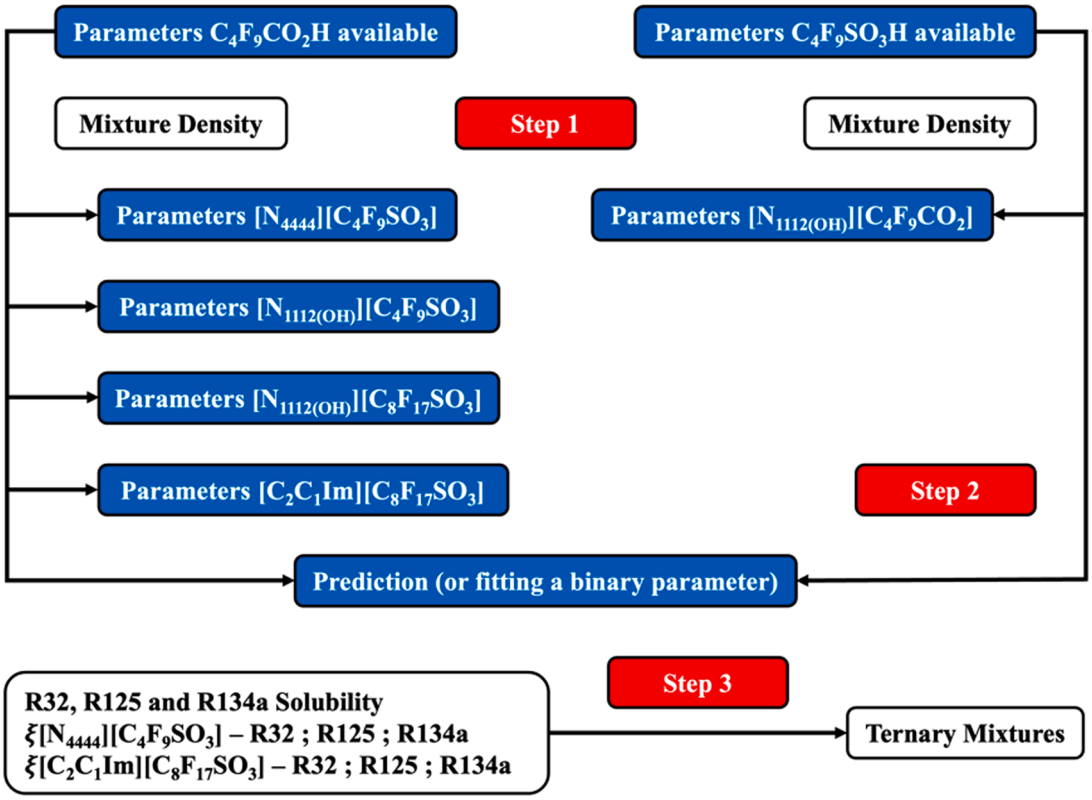

Fig. 1. Schematic procedure indicating the steps followed to optimise the molecular parameters of different HBAs forming FDESs involved in this study.

Table 1
soft-SAFT molecular parameters of the HFCs, salts and acids supporting the DESs using the individual-component model.

Compound	M_w (g/mol)	m	σ (Å)	ε/k_B (K)	ε^{HB}/k_B (K)	K^{HB} (Å^3)
$[N_{4444}][C_4F_9SO_3]$	541.56	6.390	4.703	331.3	3850	2250
$[C_2C_1Im][C_8F_{17}SO_3]$	610.29	5.734	4.534	293.2	3450	2250
$[N_{1112(OH)}][C_4F_9SO_3]$	403.26	8.411	3.647	360.8	3850	2250
$[N_{1112(OH)}][C_4F_9CO_2]$	367.21	8.263	3.634	370.1	3850	2250
$[N_{1112(OH)}][C_8F_{17}SO_3]$	603.29	10.346	3.809	367.5	3450	2250
$[C_4F_9CO_2H]$ [53]	264.05	2.403	4.550	298.5	2200	2250
$[C_4F_9SO_3H]$ [53]	300.09	2.403	4.652	302.9	2200	2250
R-32 [33]	52.02	1.321	3.529	144.4	1708	24050
R-125 [33]	120.02	1.392	4.242	148.8	1685	24050
R-134a [54]	102.03	1.392	4.166	166.6	1862	24050

capture the complexities of molecular interactions, particularly those associated with polar interactions, so as to accurately capture both, enthalpic and entropic effects. Similar methodologies have been employed in previous works using soft-SAFT, which modelled the interaction of F-gases with FILs [20,40,53] and the interaction between DES and F-gases [53]. The rest of possible binary parameters (i.e. the salt-acid and the acid-refrigerant) are kept equal to one (which means that no correction applies) in an effort to reduce the number of parameters and increase the transferability of the approach [53]. For each DES, the intermediate temperature isotherm was used to obtain optimal ξ and η values, while the other two isotherms were predicted. A summary of the binary parameters found for all DESs with the three studied refrigerants is summarised in Table 2.

As it can be seen, the effect of the energy binary parameter was found to be slightly dependent on the eutectic composition, while a constant size binary parameter was good enough to obtain quantitative agreement. The values of these parameters are related to the interactions between the various mixtures and conditions studied. Overall, a value of the energy and size binary parameters greater than 1 is found, indicating that the crossed size and dispersive energy interactions between the salt and the refrigerants are underpredicted when using the non-modified Lorentz-Berthelot combining rules.

In the next subsections, we aim to provide a careful analysis of the solubility of the refrigerants in the selected DESs, by describing the performance of the soft-SAFT model and the impact of the studied DESs features on the solubility.

4.2.1. *Effect on the HBA:HBD ratio*

Aiming to assess the effect of the proportion between the salt and the carboxylic acid on the solubility of the refrigerant, the $[N_{4444}][C_4F_9SO_3]$ salt, acting as HBA, is combined with the $[HC_4F_9CO_2]$, acting as HBD, at different proportions, forming the DES A = $[N_{4444}][C_4F_9SO_3]$:$[HC_4F_9CO_2]$. As mentioned, the only parameters fitted are the refrigerant + salt interactions. In Fig. 3, the pressure-composition diagrams show the solubility of the three refrigerants under study in DES A at three different proportions (1:1), (1:2), and (2:1) and at a selected intermediate temperature of 313.15 K. For the three studied refrigerants, the highest F-gas solubilities are observed at a ratio (2:1).

In terms of modelling, the only values largely differing from one were those describing the interaction with R-125, reaching similar numbers to those obtained in previous contributions, where this refrigerant was modelled using fluorinated ionic liquids [20,33,53]. The rest are close to the unity, indicating that fully predictive calculations would be able to qualitatively describe the system as well. This is a relevant feature of the proposed model when considering the possibility of exploring other proportions where data may not be available. The results obtained with

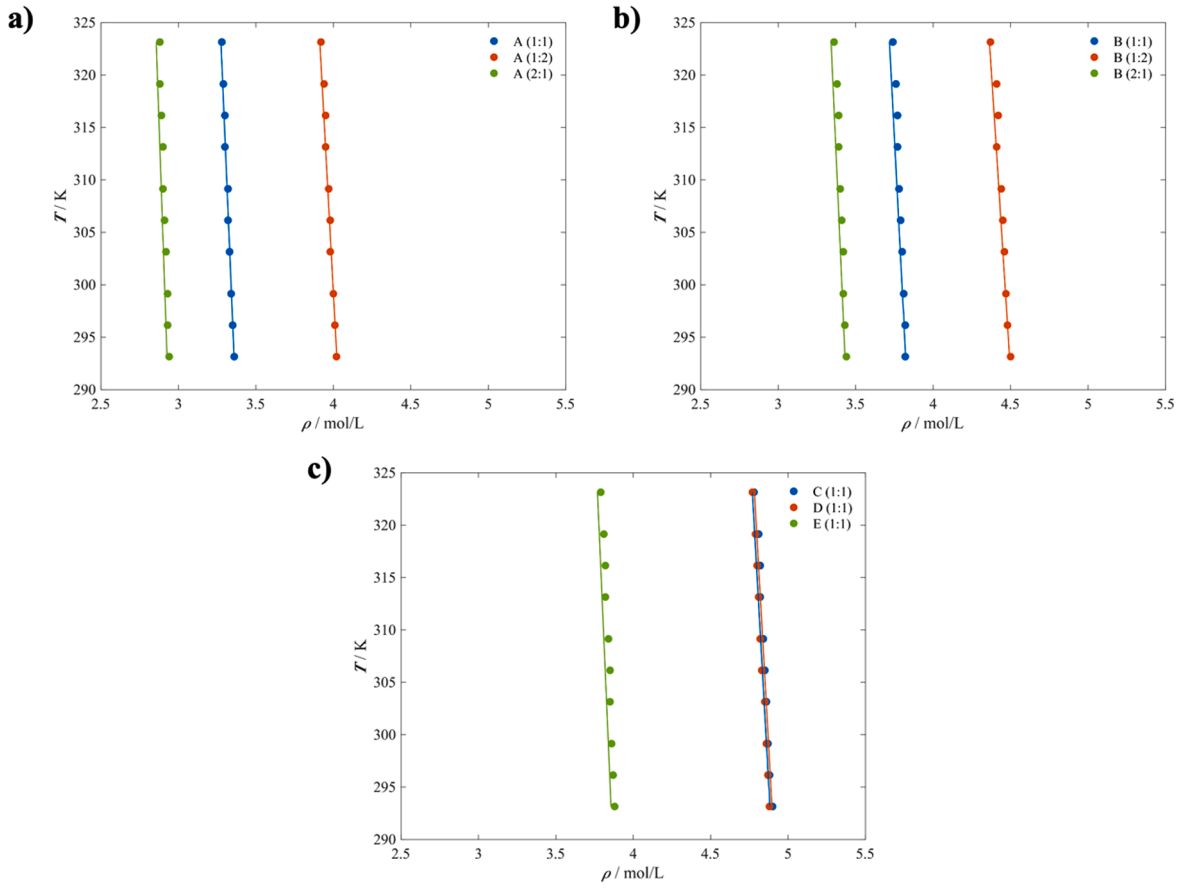

Fig. 2. Temperature-density diagrams using the individual-component approach for the following DES **a)** A (1:1) (blue circles); A (1:2) (red circles) and A (2:1) (green circles), **b)** B (1:1) (blue circles), B(1:2) (red circles), B (2:1) (green circles). **c)** C (1:1) (blue circles), D (1:1) (red circles), E(1:1) (green circles). In all figures, symbols are experimental data from Castro et al. [26], while the lines correspond to soft-SAFT calculations.

Table 2
Binary Energy and Size Parameters between R-32, R-125, and R-134a and salt binary pairs[a].

Binary pair / HBA:HBD ratio	η	ξ		
	any	1:2	1:1	2:1
$[N_{4444}][C_4F_9SO_3]$[b] + R-134a	1.018	0.990	1.000	1.030
$[N_{4444}][C_4F_9SO_3]$[b] + R-32	1.052	1.028	1.060	1.070
$[N_{4444}][C_4F_9SO_3]$[b] + R-125	1.040	1.125	1.140	1.149
$[C_2C_1Im][C_8F_{17}SO_3]$[b] + R-134a	0.990	1.000	1.000	1.000
$[C_2C_1Im][C_8F_{17}SO_3]$[b] + R-32	1.052	0.990	1.020	1.030
$[C_2C_1Im][C_8F_{17}SO_3]$[b] + R-125	1.040	1.085	1.100	1.115
$[N_{1112(OH)}][C_4F_9SO_3]$ [b] + R-134a	1.018		1.100	
$[N_{1112(OH)}][C_4F_9CO_2]$[c] + R-134a	1.070		1.130	
$[N_{1112(OH)}][C_8F_{17}SO_3]$ [b] + R-134a	1.140		1.060	

[a] A value equal to 1 means that the parameter is not necessary (no modification of the original LB combining rule).
[b] HBD of the DES is $[HC_4F_9CO_2]$.
[c] HBD of the DES is $[C_4F_9SO_3H]$.

soft-SAFT are in good agreement with the available experimental data, with the exception of the 1:2 proportion for the solubility of R-134a in DES A, where the model overpredicts the experimental behaviour. Similar results are obtained for $[N_{4444}][C_4F_9SO_3]$:$[HC_4F_9SO_3]$ and $[C_2C_1Im][C_8F_{17}SO_3]$:$[HC_4F_9CO_2]$ at 303.15 K, plotted in **Figures S3** and **S4** of the Supplementary Information, respectively. In **Figure S3e,** the solubility of $[C_2mim][C_4F_9CO_2]$, a similar IL (the cation is modified to make the salt liquid) has been added for comparative purposes. The results obtained are very promising when comparing the DESs solubility with the IL [53]. The addition of more fluorinated chains seems to improve the solubility power for R-134a. The highest solubility of R-134a is found when using $[N_{4444}][C_4F_9SO_3]$:$[HC_4F_9SO_3]$ at 2:1 and 1:1 ratios, compared to $[C_2mim][C_4F_9CO_2]$ (see **Figure S3e**).

4.2.2. *Effect of the temperature*

The effect of the temperature on the solubility of the refrigerant was also assessed. To illustrate this effect, the solubility of R-134a in $[N_{4444}][C_4F_9SO_3]$:$[HC_4F_9CO_2]$ at a 2:1 ratio was described at three temperatures and plotted in Fig. 4. The soft-SAFT calculations for the system R-134a + $[N_{4444}][C_4F_9SO_3]$:$[HC_4F_9CO_2]$ (2:1) show good agreement with the experimental data [26]. The solubility decrease with the increase of temperature is properly captured by the model, without the necessity of additional fitting. Here, it is important to remind that the binary parameters $\xi = 1.030$ and $\eta = 1.018$ (see Table 2) were fitted to an intermediate isotherm at 313.15 K and used to predict the behaviour at the remaining temperatures. A similar behaviour was also obtained for the solubility of R-32 and R-125 in DES A at a 2:1 ratio (see **Figure S3**), as well as for other HBA:HBD proportions for the solubility of R-134a in $[C_2C_1Im][C_8F_{17}SO_3]$ (ratio 1:1), provided in **Figure S4** in the Supplementary Information.

4.2.3. *Effect of the refrigerant*

The solubility of different types of refrigerants, i.e., R-134a, R-32, and R-125, was now compared considering $[N_{4444}][C_4F_9SO_3]$:$[HC_4F_9CO_2]$ in a 1:1 ratio at the lowest temperature (highest solubility) of 303.15 K. The results are plotted in Fig. 5. R-134a is the F-gas having the highest solubility, followed by R-125 and R-32, which behave very

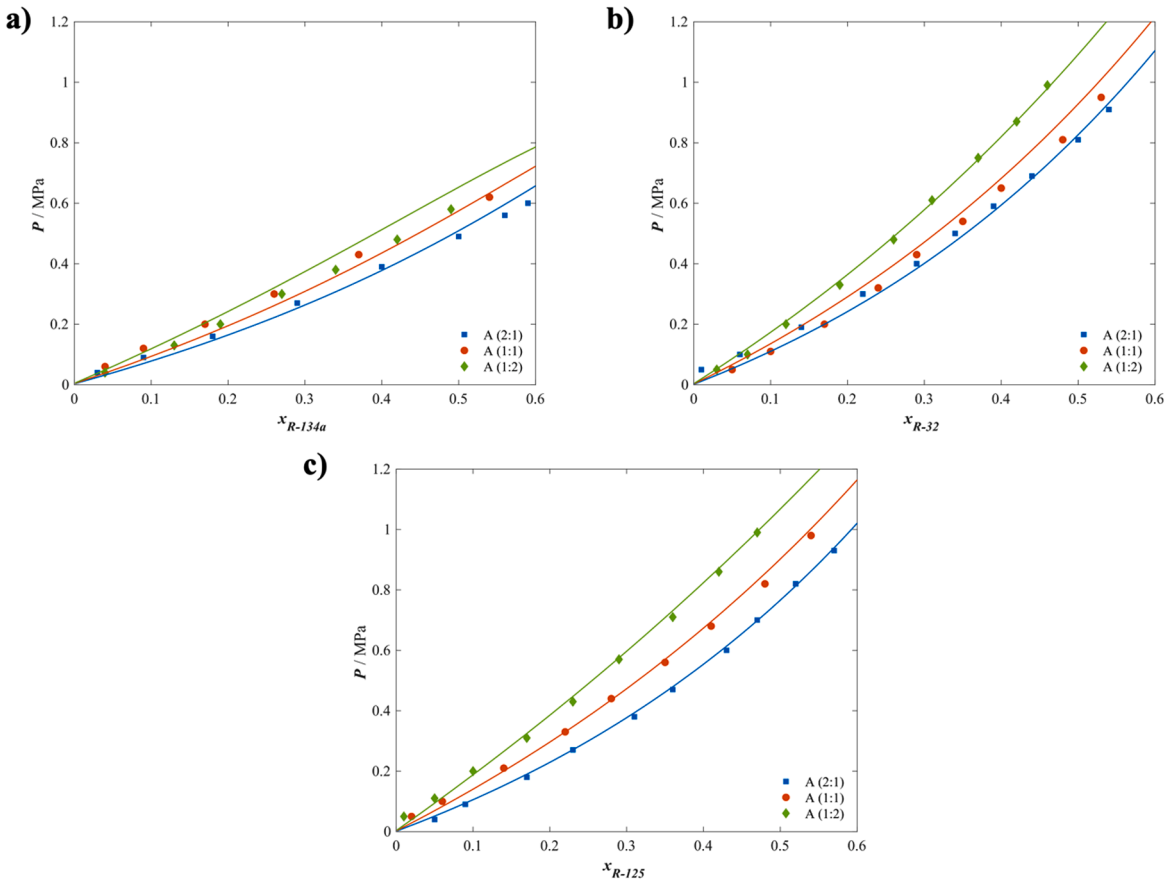

Fig. 3. Pressure-composition diagram at 313.15 K of **a)** R-134a, **b)** R-32, and **c)** R-125 with $[N_{4444}][C_4F_9SO_3]$:$[HC_4F_9CO_2]$ 1:1 (red circles), $[N_{4444}][C_4F_9SO_3]$:$[HC_4F_9CO_2]$ 1:2 (green diamonds), $[N_{4444}][C_4F_9SO_3]$:$[HC_4F_9CO_2]$ 2:1 (blue squares) Symbols represent the experimental data from Castro et al. [26] and lines correspond to the soft-SAFT calculations.

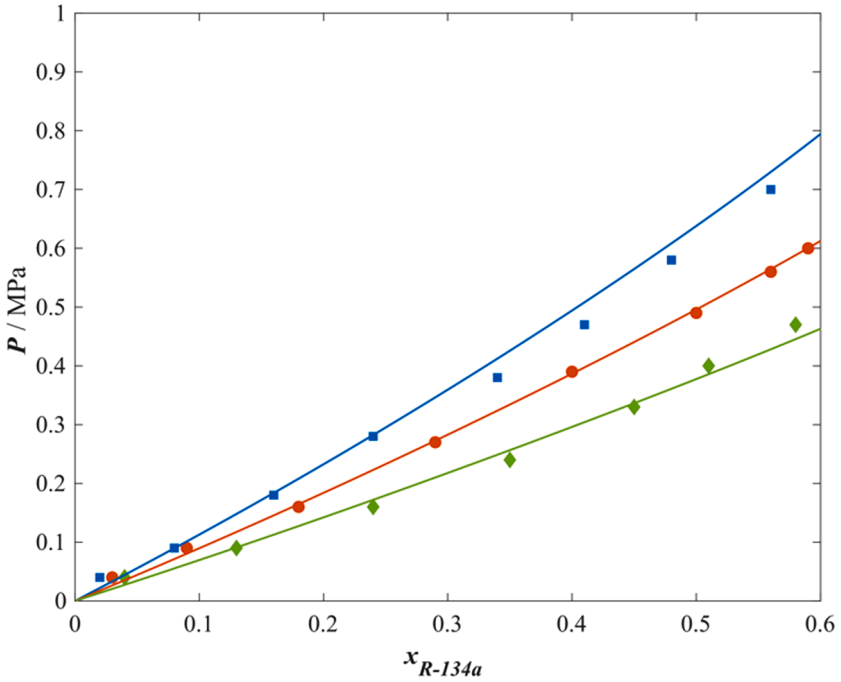

Fig. 4. Pressure-composition diagram of the solubility of R-134a in $[N_{4444}][C_4F_9SO_3]$:$[HC_4F_9CO_2]$ 2:1 at 303.15 K (green diamonds), 313.15 K (red circles), and 323.15 K (blue squares). Symbols represent the experimental data from Castro et al. [26] and lines correspond to soft-SAFT calculations.

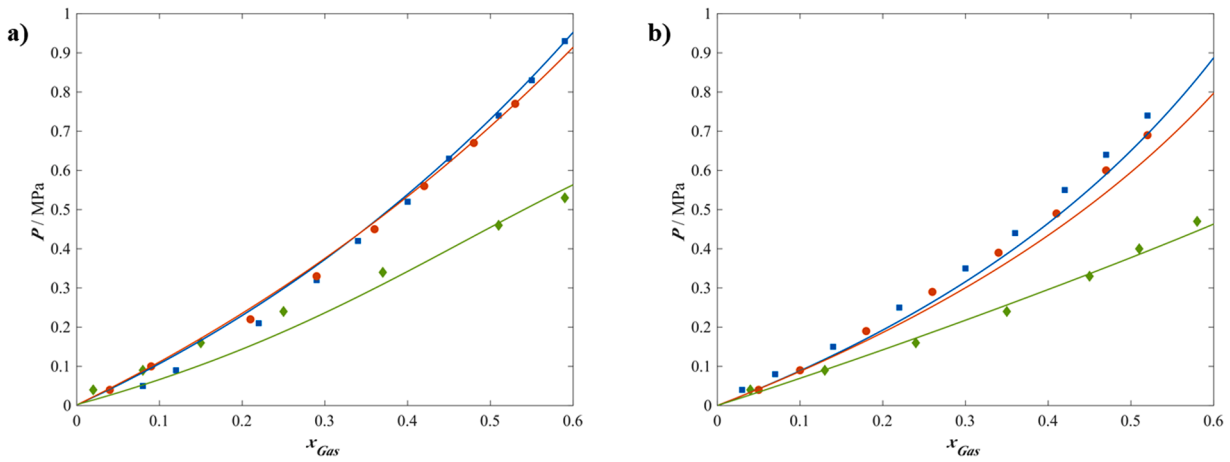

Fig. 5. Pressure-composition diagram of de solubility of R-32 (blue squares), R-125 (red circles), and R-134a (green diamonds) in $[N_{4444}][C_4F_9SO_3]$:$[HC_4F_9CO_2]$ at 303.15 K. **a)** 1:1 ratio and **b)** 2:1 ratio. Symbols represent the experimental data from Castro et al. [26], and the lines correspond to soft-SAFT calculations.

similarly. This is an indication of the difficulty of separating R-32 from R-125 using this DES at the selected proportion, as it will be shown in subsection 4.3. These results can be related to the proportion of fluorine/hydrogen atoms present in the F-gas structure. As far as these refrigerants can form hydrogen bonds (H-F-H) with a DES, hydrogen-containing fluorocarbons have a higher solubility.

Regarding the soft-SAFT predictions, the agreement is very good in all cases. Here, the parameters, ξ and η, fitted to data at 313.15K, were used in a predictive manner at 303.15 K. The behaviour of these parameters follows a similar pattern, regardless of the F-gas, with ξ showing a slight composition dependence. As noted before, R-125 parameters exhibit higher values, indicating a stronger underprediction of the interactions.

4.2.4. *Effect of the DES type*

Finally, the influence of the structure of the DES on the F-gas solubility is assessed in Fig. 6. $[N_{4444}][C_4F_9SO_3]$:$[HC_4F_9CO_2]$ and $[C_2C_1Im][C_8F_{17}SO_3]$:$[HC_4F_9CO_2]$ are considered to evaluate the impact of the addition of more fluorine atoms within the anion.

Fig. 6a shows the solubility of R-134a in DESs A and B at a 2:1 ratio and 303.15 K. As it can be seen, the more fluorinated DES B exhibits a lower solubility. While these results may sound contradictory to the idea that increasing the fluorination will improve the solubility, the imidazolium cation in DES B appears to have a negative effect compared to the ammonium cation in DES A in terms of solubility, possibly due to entropic effects. Still, it is important to mention that the differences are not significant, and the choice of the best solvent will be driven in terms of selectivity and not solubility. An additional comparison is performed at a 1:1 ratio, including also DES C, D, and E in Fig. 6b. In all cases, these alternative DESs exhibit a lower solubility of R-134a. When comparing the solubility of DES A, C, and D, which have the same number of fluorine atoms in the anion, the tetrabutylammonium cation in DES A clearly favours R-134a solubility when compared to the (2-hydroxyethyl)trimethylammonium cation in DESs C and D.

Regarding the soft-SAFT modelling of $[C_2C_1Im][C_8F_{17}SO_3]$:$[HC_4F_9CO_2]$ + F-gas systems, only the salt + refrigerant interactions are fitted, as done before. The adjusted parameters, shown in Table 2, are similar to those obtained for $[N_{4444}][C_4F_9SO_3]$:$[HC_4F_9CO_2]$ and close to unity. In general, it is observed that a coarse-grain approach can accurately describe F-gas solubility in these systems.

4.3. *Selectivity and Selection of Best Solvent*

From the description of the solubility of R-134a, R-32, and R-125 in previous DESs at different proportions and temperatures, the selectivity of these solvents to separate the refrigerants is predicted through soft-SAFT EoS. As a first approach, the ideal selectivity is evaluated without considering the effect of including all refrigerants at the same

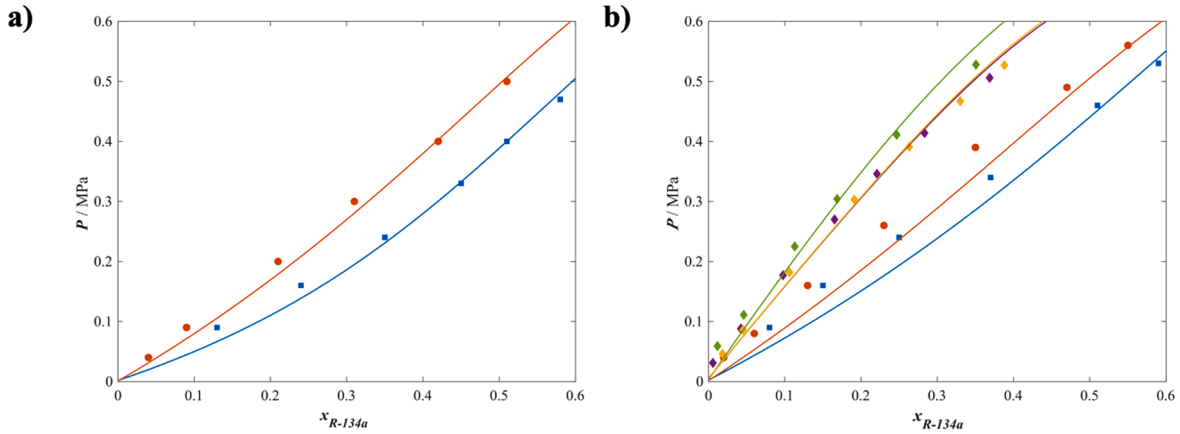

Fig. 6. Pressure-composition diagram of de solubility of R-134a in the studied DESs at 303.15 K. **a)** ratio (2:1) DES A (blue squares), DES B (red circles) and **b)** ratio (1:1) for DES A (blue squares), DES B (red circles) DES C (yellow diamonds), DES D (purple diamonds), DES E (green diamonds). Symbols represent the experimental data from Castro et al. [26], and the lines correspond to soft-SAFT calculations. Notice that predictions for DESs C and D are almost overlapped in this projection.

time (competitive selectivity). Still, it becomes a starting point to make comparisons of the most promising solvent. The ideal selectivity at infinite dilution, denoted as α, is defined as the ratio of effective Henry's law constants [58] of the two pure refrigerants i and j in the DES. It represents the amount of refrigerant gas dissolved in the DES, considering it as composed of two individual compounds within the individual-component approach, at a constant temperature [36].

$$\alpha_{i/j}\big|_T = \frac{H_{j,DES,eff}\big|_T}{H_{i,DES,eff}\big|_T} = \frac{\lim_{x_j\to 0}\left(\frac{P}{x_j}\right)\Big|_T}{\lim_{x_i\to 0}\left(\frac{P}{x_i}\right)\Big|_T} \tag{6}$$

where T and P refer to the absolute temperature and pressure, respectively. $H_{i,DES,eff}|_T$ is effective Henry's law constant for compound i at temperature T, x_i is the composition of compound i, and $\alpha_{i/j}$ represents the ideal selectivity at infinite dilution of compound j, with regard to compound i at temperature T.

The soft-SAFT EoS is used to estimate pressure data as solubility approaches zero for each isotherm and to calculate the appropriate selectivity for the blend in terms of volatility or effective Henry's law constants.

Other additional properties of interest to evaluate the capacity of DESs as solvents for refrigerant separation are the entropy and enthalpy of dissolution, commonly evaluated at fixed composition as:

$$\Delta H_{dis} = R\left(\frac{\partial ln\ P_{refrigerant}}{\partial(1/T)}\right)_{x_{refrigerant}} \tag{7}$$

$$\Delta S_{dis} = -R\left(\frac{\partial ln\ P_{refrigerant}}{\partial ln\ T}\right)_{x_{refrigerant}} \tag{8}$$

In particular, the enthalpy of dissolution provides information of the energy required to absorb (or desorb) the refrigerant, and it is related to the energy requirements of the system. All these properties have been calculated through soft-SAFT and are reported for all studied systems in **Tables S1** and **S2** in the Supplementary Information. Effective Henry's constants were calculated from the slope of the R-134a, R-32, and R-125 solubility curves, i.e., the corresponding pressure vs mole fraction of F-gas diagram at the limit of infinite dilution of the dissolved refrigerant and at three different temperatures. The values of H_i were obtained in the range of low gas composition (0.01 to 0.05 of $x_{F\text{-}gas}$) corresponding to the infinite dilution of each F-gas in DES. A smaller value of H_i corresponds to a larger absorption of F-gas by the FDES. In this sense, lower values of H_i were found for all DES in the case of R-134a refrigerant, being the smallest value for $[N_{4444}][C_4F_9SO_3]$:$[HC_4F_9CO_2]$ DES in ratio 2:1 at all considered temperatures. Moreover, this DES was the only one to display H_i values lower than unity for all tested refrigerants at 303.15 K, having a higher solvent capacity. Concerning the results achieved for the enthalpy of dissolution of R-134a, the exothermic character of the solution is shown for $[N_{4444}][C_4F_9SO_3]$:$[HC_4F_9CO_2]$ (~ –23 to –25 kJ mol^{-1}). These values are acceptable considering that there is not any chemisorption process involved. Furthermore, the molar entropies of absorption of R-134a in this DES are in a range between ~ –74 to –80 J mol^{-1}·K^{-1}, slightly decreasing when increasing the molar ratio of the salt. The results for the enthalpies of dissolution of R-32 and R-125 are quite similar, and the exothermic behaviour of the solution is shown (~ –16 to –20 kJ mol^{-1}) for $[N_{4444}][C_4F_9SO_3]$:$[HC_4F_9CO_2]$. This range of values correlate to physical absorption and is significantly lower than the enthalpies obtained when CO_2 [59] is solubilised in amines (~ –80 kJ mol^{-1}), showing that the energetic regeneration costs of these DESs might be low.

Based on Effective Henry's constants, the selectivity of R-32/R-125, R-134a/R-125, and R-134a/R-32 at 303.15 K is reported in Fig. 7. According to these results, the separation of R-125 and R-32 from R-134a (orange and blue columns, respectively) seems feasible with the (1:2) proportion for both DES $[C_2C_1Im][C_8F_{17}SO_3]$:$[HC_4F_9CO_2]$ and $[N_{4444}][C_4F_9SO_3]$:$[HC_4F_9CO_2]$, with selectivity values around 2, being DES B slightly better for R-125. Here, it is important to note that the solubility of the refrigerants in the DESs with a (1:2) ratio was slightly worse than in other proportions (see the corresponding H_i values at 303.15 K in Table S1 in the Supplementary Information). However, these DESs offer the best capacity to separate both compounds of R-134a according to selectivity calculations.

Concerning the R-32 and R-125 separation, none of the studied

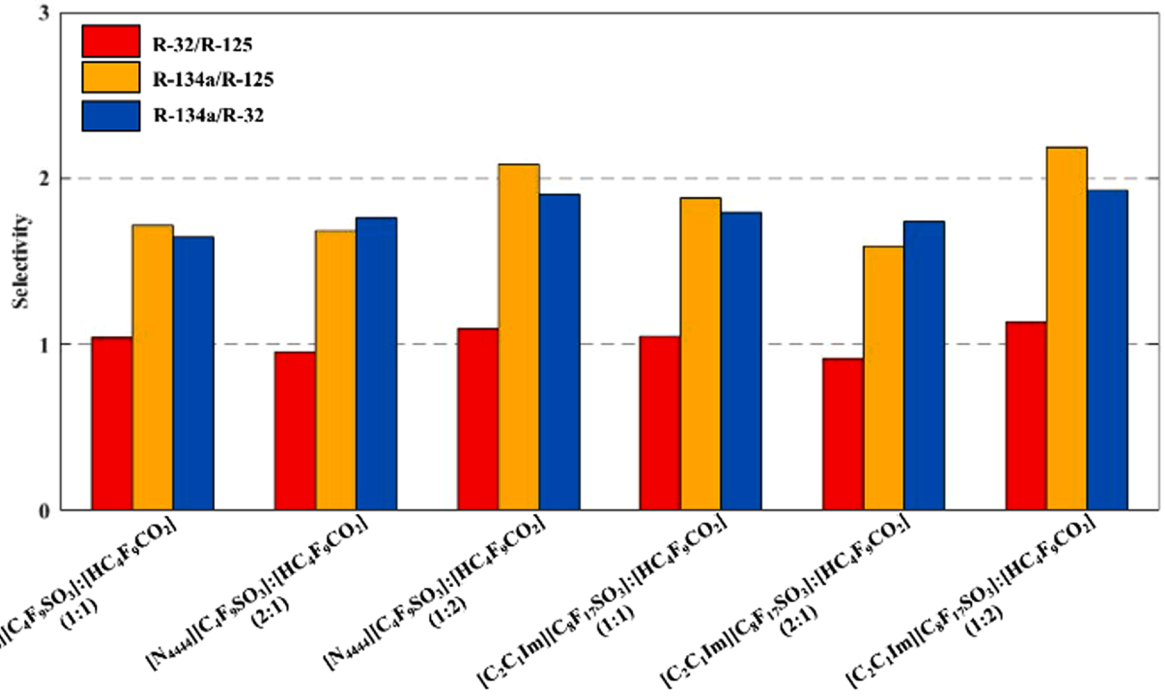

Fig. 7. Ideal selectivities at 303.15 K, calculated from effective Henry's constants from soft-SAFT, for the DES A and B.

possibilities is good because all DESs selectivities calculated have a value around 1, as shown by red columns in Fig. 7, so there is no preference in absorbing any compound. In this case, the best option would be $[C_2C_1Im][C_8F_{17}SO_3]$:$[HC_4F_9CO_2]$ (1:2), whose value is slightly above 1, but other solvents should be studied to carry out a successful separation of these two refrigerants. The selectivity values at 313.15 and 323.15 K are shown in **Figure S5** in the Supplementary Information for all cases, providing similar conclusions.

5. Conclusions

In this work, molecular models based on soft-SAFT approach have been developed and used to represent the thermodynamic behaviour of five fluorinated DESs, derived from perfluorinated acids ($C_4F_9CO_2H$ and $C_4F_9SO_3H$) and fluorinated salts, and to evaluate their capacity to absorb F-refrigerants. For this purpose $[N_{4444}][C_4F_9SO_3]$, $[C_2C_1Im][C_8F_{17}SO_3]$, $[N_{1112(OH)}][C_4F_9SO_3]$, $[N_{1112(OH)}][C_4F_9CO_2]$, and $[N_{1112(OH)}][C_8F_{17}SO_3]$ were modelled using the soft-SAFT EoS. The individual-component approach was used to develop molecular models for these salts (considering experimental data for FDESs) since all parameters became composition-independent, providing more flexibility and transferability for the proposed models. The proposed parametrisation accurately describes the density of FDESs, evidencing the strength of soft-SAFT approach.

As the salts and F-gases have more complex interactions than the other binary combinations (i.e., acid-F-gas and salt-acid), a fixed binary size parameter and a composition-dependent energy parameter were used for the salt + F-gases pairs, while the rest of combinations were calculated without further adjustment. Once the parametrization of all systems was performed, the soft-SAFT approach was employed as a screening tool to showcase the influence of the molecular structure of the FDES and F-gases, and to address the impact of temperature and composition of the solvent on the absorption capacity of FDES.

The solubility of the F-gases in these FDES was successfully captured by soft-SAFT in all cases. The highest solubilities for all F-gases were observed for $[N_{4444}][C_4F_9SO_3]$:$[HC_4F_9SO_3]$ at a ratio 2:1. Moreover, R-134a at the lowest temperature exhibited the highest solubility in all tested DESs over a wide range of operating pressures out of the three gases studied. In terms of modelling, all binary parameters were found to be slightly higher than one, revealing that the combining rule utilised is underpredicting the crossed interaction between the DES and the refrigerant. Still, similar values were found, regardless of the temperature, allowing a good description at all operating conditions.

From these models, effective Henry's constants, enthalpy and entropy of dissolution, and ideal selectivity values were calculated. While $[C_2C_1Im][C_8F_{17}SO_3]$:$[HC_4F_9CO_2]$ (1:2), closely followed by $[N_{4444}][C_4F_9SO_3]$:$[HC_4F_9CO_2]$ (1:2), were the best candidates to separate R-134a from the other two refrigerants, none of the options evaluated seems to be suitable for the R-32 / R-125 separation. Still, it is possible to adjust the selectivity towards each F-gas at lower pressures by modifying the composition ratio of each DES and the operating temperature.

This work emphasizes the capability of molecular-based equations of state, such as soft-SAFT, to screen the capacity of new solvents in terms of gases solubility and selectivity in a quick and efficient manner, becoming a useful tool for solvent selection.

CRediT authorship contribution statement

Merve Gözdenur Demirbek: Writing – original draft, Investigation, Formal analysis. **Sabrina Belén Rodriguez Reartes:** Writing – review & editing, Formal analysis. **Fèlix Llovell:** Writing – review & editing, Supervision, Software, Resources, Project administration, Methodology, Investigation, Funding acquisition, Formal analysis, Conceptualization.

Declaration of competing interest

The authors declare that they have no known competing financial interests or personal relationships that could have appeared to influence the work reported in this paper.

Data availability

Data will be made available on request.

Acknowledgements

This work has been performed in the framework of project PID2019-108014RB-C21 funded by the Spanish Ministry of Science and Innovation (MCIN/AEI/10.13039/501100011033). Additional support has been provided by project TED2021-130959B-I00, also funded by MCIN/AEI/10.13039/501100011033 and by the European Union NextGenerationEU/ PRTR. S.B. Rodriguez-Reartes acknowledges the financial support of the "María Zambrano" grant awarded by Universitat Rovira i Virgili for the requalification of the Spanish university system for 2021-2023. Additional funding from AGAUR as a Consolidated Research Group (SGR 2021-00738) is gratefully acknowledged.

Supplementary materials

Supplementary material associated with this article can be found, in the online version, at doi:10.1016/j.fluid.2024.114077.

References

[1] Intergovernmental Panel on Climate Change, Summary for Policymakers, Climate Change 2013-The Physical Science Basis: Working Group I Contribution to the Fifth Assessment Report of the Intergovernmental Panel on Climate Change, Cambridge University Press, Cambridge, 2014, pp. 1–30. Cambridge University Press.
[2] EEA greenhouse gases — data viewer. Data viewer on greenhouse gas emissions and removals, sent by countries to UNFCCC and the EU Greenhouse Gas Monitoring Mechanism, European Environment Agency, EU Member States, 2023.
[3] European Union, Regulation (EU) No 517/2014 of the European Parliament and of the Council of 16 April 2014 on Fluorinated Greenhouse Gases and Repealing Regulation (EC) No 842/2006 Text with EEA, 2014.
[4] A.A. Lindley, A. McCulloch, Regulating to reduce emissions of fluorinated greenhouse gases, J Fluor Chem 126 (2005) 1457–1462, https://doi.org/10.1016/j.jfluchem.2005.09.011.
[5] United Nations, Handbook for the Montreal Protocol on Substances that Deplete the Ozone Layer, 9th ed., Ozone Secretariat, U.N., 2012.
[6] E.A. Heath, Amendment to the Montreal Protocol on Substances that Deplete the Ozone Layer (Kigali Amendment), International Legal Materials 56 (2017) 193–205, https://doi.org/10.1017/ilm.2016.2.
[7] G.J.M. Velders, J.S. Daniel, S.A. Montzka, I. Vimont, M. Rigby, P.B. Krummel, J. Muhle, S. O'Doherty, R.G. Prinn, R.F. Weiss, D. Young, Projections of hydrofluorocarbon (HFC) emissions and the resulting global warming based on recent trends in observed abundances and current policies, Atmos Chem Phys 22 (2022) 6087–6101, https://doi.org/10.5194/acp-22-6087-2022.
[8] J.E. Sosa, C. Malheiro, R.P. Ribeiro, P.J. Castro, M.M. Piñeiro, J.M. Araújo, F. Plantier, J.P. Mota, A.B. Pereiro, Adsorption of fluorinated greenhouse gases on activated carbons: evaluation of their potential for gas separation, Journal of Chemical Technology & Biotechnology 95 (2020) 1892–1905, https://doi.org/10.1002/jctb.6371.
[9] B.S. Akkimaradi, M. Prasad, P. Dutta, K. Srinivasan, Adsorption of 1,1,1,2-Tetrafluoroethane on Activated Charcoal, J Chem Eng Data 46 (2001) 417–422, https://doi.org/10.1021/je000277e.
[10] M. Ghazy, K. Harby, A.A. Askalany, B.B. Saha, Adsorption isotherms and kinetics of activated carbon/Difluoroethane adsorption pair: Theory and experiments, International Journal of Refrigeration 70 (2016) 196–205, https://doi.org/10.1016/j.ijrefrig.2016.01.012.
[11] B.B. Saha, I.I. El-Sharkawy, R. Thorpe, R.E. Critoph, Accurate adsorption isotherms of R134a onto activated carbons for cooling and freezing applications, International Journal of Refrigeration 35 (2012) 499–505, https://doi.org/10.1016/j.ijrefrig.2011.05.002.
[12] F. Pardo, G. Zarca, A. Urtiaga, Separation of Refrigerant Gas Mixtures Containing R32, R134a, and R1234yf through Poly(ether- *block* -amide) Membranes, ACS Sustain Chem Eng 8 (2020) 2548–2556, https://doi.org/10.1021/acssuschemeng.9b07195.
[13] J.E. Sosa, R.P.P.L. Ribeiro, P.J. Castro, J.P.B. Mota, J.M.M. Araújo, A.B. Pereiro, Absorption of Fluorinated Greenhouse Gases Using Fluorinated Ionic Liquids, Ind

Eng Chem Res 58 (2019) 20769–20778, https://doi.org/10.1021/acs.iecr.9b04648.
[14] M.B. Shiflett, A. Yokozeki, Solubility Differences of Halocarbon Isomers in Ionic Liquid [emim][Tf $_2$ N], J Chem Eng Data 52 (2007) 2007–2015, https://doi.org/10.1021/je700295e.
[15] L. Dong, D. Zheng, G. Sun, X. Wu, Vapor–Liquid Equilibrium Measurements of Difluoromethane + [Emim]OTf, Difluoromethane + [Bmim]OTf, Difluoroethane + [Emim]OTf, and Difluoroethane + [Bmim]OTf Systems, J Chem Eng Data 56 (2011) 3663–3668, https://doi.org/10.1021/je2005566.
[16] M.B. Shiflett, M.A. Harmer, C.P. Junk, A. Yokozeki, Solubility and Diffusivity of Difluoromethane in Room-Temperature Ionic Liquids, J Chem Eng Data 51 (2006) 483–495, https://doi.org/10.1021/je050386z.
[17] X. Liu, M. He, N. Lv, X. Qi, C. Su, Solubilities of R-161 and R-143a in 1-Hexyl-3-methylimidazolium bis(trifluoromethylsulfonyl)imide, Fluid Phase Equilib 388 (2015) 37–42, https://doi.org/10.1016/j.fluid.2014.12.026.
[18] M.B. Shiflett, A. Yokozeki, Binary Vapor–Liquid and Vapor–Liquid–Liquid Equilibria of Hydrofluorocarbons (HFC-125 and HFC-143a) and Hydrofluoroethers (HFE-125 and HFE-143a) with Ionic Liquid [emim][Tf $_2$ N], J Chem Eng Data 53 (2008) 492–497, https://doi.org/10.1021/je700588d.
[19] W. Ren, A.M. Scurto, Phase equilibria of imidazolium ionic liquids and the refrigerant gas, 1,1,1,2-tetrafluoroethane (R-134a), Fluid Phase Equilib 286 (2009) 1–7, https://doi.org/10.1016/j.fluid.2009.07.007.
[20] M.L. Ferreira, J.M.M. Araújo, L.F. Vega, A.B. Pereiro, Understanding the Absorption of Fluorinated Gases in Fluorinated Ionic Liquids for Recovering Purposes Using Soft-SAFT, J Chem Eng Data 67 (2022) 1951–1963, https://doi.org/10.1021/acs.jced.1c00984.
[21] M.B. Shiflett, A. Yokozeki, Solubility and diffusivity of hydrofluorocarbons in room-temperature ionic liquids, AIChE Journal 52 (2006) 1205–1219, https://doi.org/10.1002/aic.10685.
[22] M.B. Shiflett, A. Yokozeki, J.P. Knapp, Process for the Separation of Fluorocarbons Using Ionic Liquids, US7,964,760B2 (2007).
[23] F.P. Pelaquim, A.M. Barbosa Neto, I.A.L. Dalmolin, M.C. da Costa, Gas Solubility Using Deep Eutectic Solvents: Review and Analysis, Ind Eng Chem Res 60 (2021) 8607–8620, https://doi.org/10.1021/acs.iecr.1c00947.
[24] G. García, S. Aparicio, R. Ullah, M. Atilhan, Deep Eutectic Solvents: Physicochemical Properties and Gas Separation Applications, Energy & Fuels 29 (2015) 2616–2644, https://doi.org/10.1021/ef5028873.
[25] V. Codera, D. Clijnk, J.O. Pou, J. Fernandez-Garcia, F. Llovell, R. Gonzalez-Olmos, Process design for the recovery of waste refrigerants using deep eutectic solvents, J Environ Chem Eng 11 (2023) 110255, https://doi.org/10.1016/j.jece.2023.110255.
[26] P.J. Castro, A.E. Redondo, J.E. Sosa, M.E. Zakrzewska, A.V.M. Nunes, J.M. M. Araújo, A.B. Pereiro, Absorption of Fluorinated Greenhouse Gases in Deep Eutectic Solvents, Ind Eng Chem Res 59 (2020) 13246–13259, https://doi.org/10.1021/acs.iecr.0c01893.
[27] M.L. Ferreira, M.J. Pastoriza-Gallego, J.M.M. Araújo, J.N. Canongia Lopes, L.P. N. Rebelo, M.M. Piñeiro, K. Shimizu, A.B. Pereiro, Influence of Nanosegregation on the Phase Behavior of Fluorinated Ionic Liquids, The Journal of Physical Chemistry C 121 (2017) 5415–5427, https://doi.org/10.1021/acs.jpcc.7b00516.
[28] L.F. Lepre, D. Andre, S. Denis-Quanquin, A. Gautier, A.A.H. Pádua, M.Costa Gomes, Ionic Liquids Can Enable the Recycling of Fluorinated Greenhouse Gases, ACS Sustain Chem Eng 7 (2019) 16900–16906, https://doi.org/10.1021/acssuschemeng.9b04214.
[29] L.F. Lepre, L. Pison, I. Otero, A. Gautier, J. Dévemy, P. Husson, A.A.H. Pádua, M. Costa Gomes, Using hydrogenated and perfluorinated gases to probe the interactions and structure of fluorinated ionic liquids, Physical Chemistry Chemical Physics 21 (2019) 8865–8873, https://doi.org/10.1039/C9CP00593E.
[30] W.G. Chapman, K.E. Gubbins, G. Jackson, M. Radosz, SAFT: Equation-of-state solution model for associating fluids, Fluid Phase Equilib 52 (1989) 31–38, https://doi.org/10.1016/0378-3812(89)80308-5.
[31] W.G. Chapman, K.E. Gubbins, G. Jackson, M. Radosz, New reference equation of state for associating liquids, Ind Eng Chem Res 29 (1990) 1709–1721, https://doi.org/10.1021/ie00104a021.
[32] F.J. Blas, L.F. Vega, Thermodynamic behaviour of homonuclear and heteronuclear Lennard-Jones chains with association sites from simulation and theory, Mol Phys 92 (1997) 135–150, https://doi.org/10.1080/002689797170707.
[33] S. Asensio-Delgado, D. Jovell, G. Zarca, A. Urtiaga, F. Llovell, Thermodynamic and process modeling of the recovery of R410A compounds with ionic liquids, International Journal of Refrigeration 118 (2020) 365–375, https://doi.org/10.1016/j.ijrefrig.2020.04.013.
[34] F. Llovell, E. Valente, O. Vilaseca, L.F. Vega, Modeling Complex Associating Mixtures with [C $_n$ -mim][Tf $_2$ N] Ionic Liquids: Predictions from the Soft-SAFT Equation, J Phys Chem B 115 (2011) 4387–4398, https://doi.org/10.1021/jp112315b.
[35] L.M.C. Pereira, M.B. Oliveira, A.M.A. Dias, F. Llovell, L.F. Vega, P.J. Carvalho, J.A. P. Coutinho, High pressure separation of greenhouse gases from air with 1-ethyl-3-methylimidazolium methyl-phosphonate, International Journal of Greenhouse Gas Control 19 (2013) 299–309, https://doi.org/10.1016/j.ijggc.2013.09.007.
[36] F. Llovell, M.B. Oliveira, J.A.P. Coutinho, L.F. Vega, Solubility of greenhouse and acid gases on the [C4mim][MeSO4] ionic liquid for gas separation and CO2 conversion, Catal Today 255 (2015) 87–96, https://doi.org/10.1016/j.cattod.2014.12.049.
[37] A.B. Pereiro, F. Llovell, J.M.M. Araújo, A.S.S. Santos, L.P.N. Rebelo, M.M. Piñeiro, L.F. Vega, Thermophysical Characterization of Ionic Liquids Based on the Perfluorobutanesulfonate Anion: Experimental and Soft-SAFT Modeling Results, ChemPhysChem 18 (2017) 2012–2023, https://doi.org/10.1002/cphc.201700327.
[38] M.L. Ferreira, F. Llovell, L.F. Vega, A.B. Pereiro, J.M.M. Araújo, Systematic study of the influence of the molecular structure of fluorinated ionic liquids on the solubilization of atmospheric gases using a soft-SAFT based approach, J Mol Liq 294 (2019) 111645, https://doi.org/10.1016/j.molliq.2019.111645.
[39] G. Alonso, P. Gamallo, R. Sayós, F. Llovell, Combining soft-SAFT and COSMO-RS modeling tools to assess the CO2–SO2 separation using phosphonium-based ionic liquids, J Mol Liq 297 (2020) 111795, https://doi.org/10.1016/j.molliq.2019.111795.
[40] C.G. Albà, L.F. Vega, F. Llovell, Assessment on Separating Hydrofluoroolefins from Hydrofluorocarbons at the Azeotropic Mixture R513A by Using Fluorinated Ionic Liquids: A Soft-SAFT Study, Ind Eng Chem Res 59 (2020) 13315–13324, https://doi.org/10.1021/acs.iecr.0c02331.
[41] I.I.I. Alkhatib, D. Bahamon, F. Llovell, M.R.M. Abu-Zahra, L.F. Vega, Perspectives and guidelines on thermodynamic modelling of deep eutectic solvents, J Mol Liq 298 (2020) 112183, https://doi.org/10.1016/j.molliq.2019.112183.
[42] J.O. Lloret, L.F. Vega, F. Llovell, Accurate description of thermophysical properties of Tetraalkylammonium Chloride Deep Eutectic Solvents with the soft-SAFT equation of state, Fluid Phase Equilib 448 (2017) 81–93, https://doi.org/10.1016/j.fluid.2017.04.013.
[43] R.M. Ojeda, F. Llovell, Soft-SAFT Transferable Molecular Models for the Description of Gas Solubility in Eutectic Ammonium Salt-Based Solvents, J Chem Eng Data 63 (2018) 2599–2612, https://doi.org/10.1021/acs.jced.7b01103.
[44] E.A. Crespo, L.P. Silva, J.O. Lloret, P.J. Carvalho, L.F. Vega, F. Llovell, J.A. P. Coutinho, A methodology to parameterize SAFT-type equations of state for solid precursors of deep eutectic solvents: the example of cholinium chloride, Physical Chemistry Chemical Physics 21 (2019) 15046–15061, https://doi.org/10.1039/C9CP02548K.
[45] L.V.T.D. Alencar, S.B. Rodriguez-Reartes, F.W. Tavares, F. Llovell, A consistent framework to characterize the impact of co-solvents in the key process thermophysical properties of choline chloride-based DESs, Journal of Industrial and Engineering Chemistry (2023), https://doi.org/10.1016/j.jiec.2023.11.021.
[46] M.S. Wertheim, Fluids with highly directional attractive forces. II. Thermodynamic perturbation theory and integral equations, J Stat Phys 35 (1984) 35–47, https://doi.org/10.1007/BF01017363.
[47] M.S. Wertheim, Fluids with highly directional attractive forces. III. Multiple attraction sites, J Stat Phys 42 (1986) 459–476, https://doi.org/10.1007/BF01127721.
[48] M.S. Wertheim, Fluids with highly directional attractive forces. IV. Equilibrium polymerization, J Stat Phys 42 (1986) 477–492, https://doi.org/10.1007/BF01127722.
[49] J.C. Pàmies, L.F. Vega, Vapor−Liquid Equilibria and Critical Behavior of Heavy *n* -Alkanes Using Transferable Parameters from the Soft-SAFT Equation of State, Ind Eng Chem Res 40 (2001) 2532–2543, https://doi.org/10.1021/ie000944x.
[50] J.K. Johnson, J.A. Zollweg, K.E. Gubbins, The Lennard-Jones equation of state revisited, Mol Phys 78 (1993) 591–618, https://doi.org/10.1080/00268979300100411.
[51] D. Henderson, P.J. Leonard, One- and Two-Fluid van der Waals Theories of Liquid Mixtures, I. Hard Sphere Mixtures, Proceedings of the National Academy of Sciences 67 (1970) 1818–1823, https://doi.org/10.1073/pnas.67.4.1818.
[52] O. Vilaseca, F. Llovell, J. Yustos, R.M. Marcos, L.F. Vega, Phase equilibria, surface tensions and heat capacities of hydrofluorocarbons and their mixtures including the critical region, J Supercrit Fluids 55 (2010) 755–768, https://doi.org/10.1016/j.supflu.2010.10.015.
[53] D. Jovell, S.B. Gómez, M.E. Zakrzewska, A.V.M. Nunes, J.M.M. Araújo, A. B. Pereiro, F. Llovell, Insight on the Solubility of R134a in Fluorinated Ionic Liquids and Deep Eutectic Solvents, J Chem Eng Data 65 (2020) 4956–4969, https://doi.org/10.1021/acs.jced.0c00588.
[54] C.G. Albà, L.F. Vega, F. Llovell, A consistent thermodynamic molecular model of n-hydrofluoroolefins and blends for refrigeration applications, International Journal of Refrigeration 113 (2020) 145–155, https://doi.org/10.1016/j.ijrefrig.2020.01.008.
[55] L.F. Zubeir, C. Held, G. Sadowski, M.C. Kroon, PC-SAFT Modeling of CO $_2$ Solubilities in Deep Eutectic Solvents, J Phys Chem B 120 (2016) 2300–2310, https://doi.org/10.1021/acs.jpcb.5b07888.
[56] M.D. Hanwell, D.E. Curtis, D.C. Lonie, T. Vandermeersch, E. Zurek, G.R. Hutchison, Avogadro: an advanced semantic chemical editor, visualization, and analysis platform, J Cheminform 4 (2012) 17, https://doi.org/10.1186/1758-2946-4-17.
[57] M. Sadeqzadeh, V. Papaioannou, S. Dufal, C.S. Adjiman, G. Jackson, A. Galindo, The development of unlike induced association-site models to study the phase behaviour of aqueous mixtures comprising acetone, alkanes and alkyl carboxylic acids with the SAFT-γ Mie group contribution methodology, Fluid Phase Equilib 407 (2016) 39–57, https://doi.org/10.1016/j.fluid.2015.07.047.
[58] R. Sander, W.E. Acree, A. De Visscher, S.E. Schwartz, T.J. Wallington, Henry's law constants (IUPAC Recommendations 2021), Pure and Applied Chemistry 94 (2022) 71–85, https://doi.org/10.1515/pac-2020-0302.
[59] L.F. Zubeir, M.H.M. Lacroix, M.C. Kroon, Low Transition Temperature Mixtures as Innovative and Sustainable CO $_2$ Capture Solvents, J Phys Chem B 118 (2014), https://doi.org/10.1021/jp5089004.